UNIVERSITY OF BIRMINGHAM

University of Birmingham Research at Birmingham

Competing charge, spin and superconducting orders in underdoped YBa2Cu3Oy

Huecker, Markus; Christensen, Niels B.; Holmes, Alexander; Blackburn, Elizabeth; Forgan, Edward; Liang, Ruixing; Bonn, D. A.; Hardy, W. N.; Gutowski, Olof; von Zimmermann, Martin ; Hayden, SM; Chang, Johan

Document Version
Publisher's PDF, also known as Version of record

[Link to publication on Research at Birmingham portal](#)

Competing charge, spin, and superconducting orders in underdoped YBa$_2$Cu$_3$O$_y$

M. Hücker,[1] N. B. Christensen,[2] A. T. Holmes,[3] E. Blackburn,[3] E. M. Forgan,[3] Ruixing Liang,[4,5] D. A. Bonn,[4,5]
W. N. Hardy,[4,5] O. Gutowski,[6] M. v. Zimmermann,[6] S. M. Hayden,[7] and J. Chang[8]

[1]*Condensed Matter Physics and Materials Science Department, Brookhaven National Laboratory, Upton, New York 11973, USA*
[2]*Department of Physics, Technical University of Denmark, DK-2800 Kongens Lyngby, Denmark*
[3]*School of Physics and Astronomy, University of Birmingham, Birmingham B15 2TT, United Kingdom*
[4]*Department of Physics and Astronomy, University of British Columbia, Vancouver, Canada V6T 1Z1*
[5]*Canadian Institute for Advanced Research, Toronto, Canada M5G 1Z8*
[6]*Deutsches Elektronen-Synchrotron DESY, 22603 Hamburg, Germany*
[7]*H. H. Wills Physics Laboratory, University of Bristol, Bristol BS8 1TL, United Kingdom*
[8]*Institut de la Materiere Complexe, Ecole Polytechnique de Lausanna (EPFL), CH-1015 Lausanne, Switzerland*

To explore the doping dependence of the recently discovered charge-density-wave (CDW) order in YBa$_2$Cu$_3$O$_y$, we present a bulk-sensitive high-energy x-ray study for several oxygen concentrations, including strongly underdoped YBa$_2$Cu$_3$O$_{6.44}$. Combined with previous data around the so-called 1/8 doping, we show that bulk CDW order exists at least for hole concentrations (p) in the CuO$_2$ planes of $0.078 \lesssim p \lesssim 0.132$. This implies that CDW order exists in close vicinity to the quantum critical point for spin-density-wave (SDW) order. In contrast to the pseudogap temperature T^*, the onset temperature of CDW order decreases with underdoping to $T_{CDW} \sim 90$ K in YBa$_2$Cu$_3$O$_{6.44}$. Together with a weakened order parameter this suggests a competition between CDW and SDW orders. In addition, the CDW order in YBa$_2$Cu$_3$O$_{6.44}$ shows the same type of competition with superconductivity as a function of temperature and magnetic field as samples closer to $p = 1/8$. At low p the CDW incommensurability continues the previously reported linear increasing trend with underdoping. In the entire doping range the in-plane correlation length of the CDW order in b axis direction depends only very weakly on the hole concentration, and appears independent of the type and correlation length of the oxygen-chain order. The onset temperature of the CDW order is remarkably close to a temperature $T^\dagger$ that marks the maximum of $1/(T_1T)$ in planar ^{63}Cu NQR/NMR experiments, potentially indicating a response of the spin dynamics to the formation of the CDW. Our discussion of these findings includes a detailed comparison to the charge stripe order in La$_{2-x}$Ba$_x$CuO$_4$.

I. INTRODUCTION

The recent observation of charge ordered ground states in Y-, Bi-, La-, and Hg-based high temperature superconductors by nuclear magnetic resonance and x-ray scattering techniques, emphasizes the need to understand the competition between these states and superconductivity in underdoped cuprates [1–10]. One of the outstanding questions is how these states are related to the Fermi surface topology. Quantum oscillation experiments on the archetypal bilayer system YBa$_2$Cu$_3$O$_y$ (YBCO) indicate a reconstruction of the large Fermi surface typical for overdoped cuprates, into one with small Fermi pockets near a hole concentration of $p \sim 1/8$ [11–18]. Similar quantum oscillation measurements in a single-layer Hg-based cuprate provide further evidence that Fermi pockets are a common property around this so-called 1/8 anomaly [19,20]. A change from positive to negative Hall and Seebeck coefficients in YBCO around this doping region led to the interpretation that the Fermi pocket must have electronlike character [21–25]. Negative Seebeck and Hall coefficients are also observed in La$_{1.8-x}$Eu$_{0.2}$Sr$_x$CuO$_4$ and several other La-based cuprates [23,24,26–31] that are known to exhibit charge and spin-stripe order [7–9,32–43]. This strongly suggested that charge and/or spin order may exist in YBCO as well [21,23,24,33,44]. Evidence of charge order was indeed revealed by NMR [1], x-ray diffraction [2,3,45–47], and ultrasound [48] experiments. However, the identified wave

vectors have been linked to a charge-density-wave (CDW) order from Fermi surface nesting rather than stripe order. In both Bi- and Hg-based cuprates the ordering wave vector was found to approximately match a nesting vector that connects the tips of the Fermi arcs, providing further support for a nesting scenario [5,6,10,49].

In spite of this tremendous progress, the connection between some of the observations remains unclear. Doping experiments may thus provide a powerful tool for further tests. Several recent studies on YBCO indicate a significant qualitative change of the electronic properties at a critical doping of approximately $p_c \sim 0.08$ [14,22,23,53–56]. In particular, the absence of a negative Seebeck and Hall effect below p_c suggests a disappearance of the proposed electron pocket, which has motivated explanations in terms of a Lifshitz transition, i.e., a transition that involves a change of the Fermi surface topology [22,23,57,58]. The region below p_c also exhibits a low-temperature spin-density-wave (SDW) order [59,60], and an electronic liquid crystal state at higher temperatures [55,61], which are reminiscent of the spin stripe phase in La-based cuprates [62]. There is no obvious relationship between the SDW order below p_c and the CDW order above p_c. In fact in YBCO, magnetic excitations are gapped in the doping region where quantum oscillations and CDW have been observed so far [63,64]. This shows that a detailed knowledge of the doping dependence of the CDW order is critical. NMR and x-ray studies have identified charge

TABLE I. Characteristic properties of the studied $YBa_2Cu_3O_y$ single crystals: oxygen content y, structure of oxygen-chain order, superconducting transition temperature T_c, hole content p, sample size, onset temperature T_{CDW} and incommensurability δ_b at T_c of the CDW order, and resolution corrected correlation lengths ξ_b of the CDW order and the chain order at T_c in the direction of the b axis. The ξ_b(CDW) value for $y = 6.54$ and the T_{CDW} values for $y = 6.54$, 6.67, and 6.75 were taken from Refs. [3,46]. ξ_b(CDW) was measured at $\mathbf{Q} = (0,\delta_b,6.5)$. ξ_b(chain) was measured at $\mathbf{Q} = (0.5,0,6)$, $(0.375,0,6)$, and $(0.333,0,6.5)$ for o-II, o-VIII, and o-III, respectively. For details related to the oxygen content y, oxygen order, and hole content p, see Refs. [50–52].

y in YBCO	Oxygen order	T_c (K)	Hole content p	Sample size $a \times b \times c$ (mm^3)	T_{CDW} (K)	δ_b (r.l.u.)	ξ_b(CDW) (Å)	ξ_b(chain) (Å)
6.44	o-II	42	0.078	$1.45 \times 1.68 \times 0.46$	90(15)	0.337(2)	51(7)	169(10)
6.512	o-II	59	0.096	$2.2 \times 1.46 \times 0.25$	145(10)	0.331(2)	61(7)	233(10)
6.54	o-II	58	0.104	$3.1 \times 1.9 \times 0.16$	155(10)	0.328(2)	66(7)	–
6.67	o-VIII	67	0.123	$3.1 \times 1.7 \times 0.6$	140(10)	0.315(2)	63(7)	138(10)
6.75	o-III	74	0.132	$3.5 \times 1.8 \times 0.5$	140(10)	0.305(4)	64(10)	116(10)
6.92	o-I	93	0.165	$1.91 \times 1.81 \times 0.57$	–	–	–	–

order down to approximately $p = 0.104$ [2,4,46]. Hence, it is still an open question how the CDW order evolves as the critical point $p_c \sim 0.08$ is approached.

Here we report a high-energy x-ray diffraction study of the CDW order in several YBCO single crystals, listed in Table I. This includes two underdoped ortho-II YBCO crystals with $y = 6.44$ and $y = 6.512$, as well as an optimally doped crystal with $y = 6.92$. While both underdoped crystals exhibit CDW order, no evidence of this order was found for $y = 6.92$. Much of the attention will concentrate on the results for $y = 6.44$, with those for $y = 6.512$ being very similar to our previous data for $y = 6.54$ [46]. The hole concentration [52] of the $YBa_2Cu_3O_{6.44}$ crystal is $p \sim 0.078$ and hence it is in close vicinity to the above mentioned quantum critical point for SDW order [55], and the proposed Lifshitz transition [22]. The CDW order in that crystal is weakened but significant and can be traced up to $T_{CDW} \sim 90$ K. Upon cooling below T_c the CDW reflection is partially suppressed, but can be enhanced by a magnetic field applied perpendicular to the CuO_2 planes. The ordering wave vector of the CDW in $YBa_2Cu_3O_{6.44}$ continues the growing trend versus underdoping previously identified around 1/8 doping [46].

Two further findings may shed light on the nature of the CDW order in YBCO. First, its correlation length ξ_b along the b axis, i.e., parallel to the chains, shows no dependence on the oxygen order in the chain layers, and varies only weakly as a function of doping, which may indicate that local properties play a role. Second, we find a remarkable agreement between the CDW onset temperature T_{CDW} and a temperature $T^\dagger$ below which $1/(T_1T)$ decreases in planar ^{63}Cu NQR/NMR experiments [56,65–70]. We argue that the opening of a CDW gap may influence the planar Cu spin dynamics. The derived phase diagrams strongly indicate that CDW order not only competes with superconductivity (SC), but also with SDW order. Finally, we discuss differences and similarities of the CDW order in YBCO and the charge stripe order in $La_{2-x}Ba_xCuO_4$ (LBCO).

II. EXPERIMENTAL DETAILS

A detailed description of the synthesis of the six flux grown YBCO single crystals with $6.44 \leqslant y \leqslant 6.92$ (cf. Table I) is given in Ref. [50]. This includes the setting and determination of the oxygen content y, the detwinning procedure, and the oxygen vacancy ordering in the chain layers. The hole concentration p in the CuO_2 planes is a unique function of T_c and the lattice parameter c, and for detwinned and well oxygen ordered crystals also a unique function of the oxygen content [52]. Since our high-energy x-ray diffraction technique is not very well suited for precision measurements of lattice constants, all p values were determined via the oxygen content and measurements of T_c. All crystals are ~99% detwinned and have sharp SC transitions, indicating well-defined carrier concentrations. Examples of the SC transition are shown in Fig. 1(d) for $y = 6.44$, 6.512, and 6.92. The crystals with $y = 6.54$, 6.67, and 6.75 are the same as in our previous studies in Refs. [3,46]. The high-energy x-ray diffraction experiments were carried out with triple-axis instruments at beamline P07 at PETRA III, DESY, and beamline 6-ID-D at the Advanced Photon Source at Argonne National Laboratory. Beamline 6-ID-D is equipped with a Ge point detector and P07 with a scintillation point detector. The beam size varied between 0.5×0.5 and 1×1 mm^2, and the photon energy was set to $E_{ph} = 80$ keV. The rectangular crystals, with dimensions listed in Table I, were mounted with the $(0,k,\ell)$ zone in the scattering plane, and studied in bulk sensitive transmission geometry. We have used the same SiGe gradient (111) analyzer crystal on all instruments, resulting in approximately the same longitudinal resolution. The transverse resolution is given by the mosaic of the single crystals, usually a few hundreds of a degree, and therefore largely independent of the instrument. Typical transverse resolution values are indicated in Figs. 1(a) and 2(b), and are significantly smaller than the width of the CDW peak. The resolution perpendicular to the scattering plane is determined by the corresponding perpendicular opening of the detector slit, and is kept at a value coarse enough to integrate a substantial part of the charge order peak in that direction. The resolution is of course q dependent. As an example we mention here the values measured at 6-ID-D and $\mathbf{Q} = (0,0,6)$, indicating a resolution of $(0.013,0.0028,0.0094)$ reciprocal lattice units (r.l.u.). The signal-to-background ratio varied between 1/3 for the strongest CDW peak for $y = 6.67$ at T_c (corresponding to 1000 cts/3000 cts in 30 s measured for $\mathbf{Q} = (0,\delta_b,6.5)$
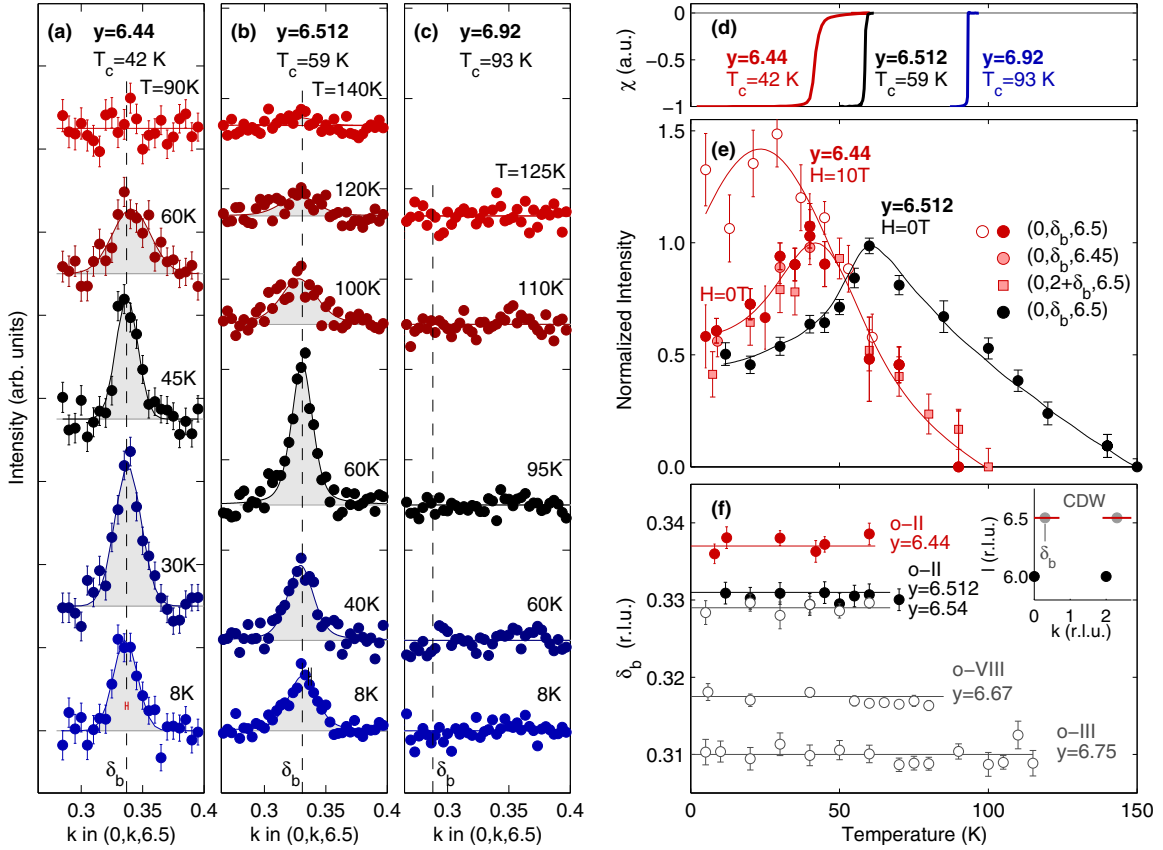
FIG. 1. (Color online) Temperature dependence of the CDW order in YBCO. (a), (b) k scans at zero magnetic field through $\mathbf{Q} = (0,\delta_b,6.5)$ for ortho-II crystals with $y = 6.44$ and 6.512, showing that the CDW order vanishes into the background noise at $T \sim 90$ K and ~ 145 K, respectively. Solid lines are least-squares fits using a Gaussian line shape. Vertical dashed lines indicate the incommensurability δ_b. (c) k scans for the optimally doped crystal with $y = 6.92$ reveal no evidence of a CDW peak. The dashed line in (c) indicates an estimated CDW peak position based on a linear extrapolation of the doping dependence $\delta_b(y)$ in Fig. 4(d). Sloping backgrounds have been subtracted from all scans that are shifted vertically for clarity. The red horizontal bar in (a) at $T = 8$ K indicates a typical transverse resolution full width at half maximum. (d) Normalized diamagnetic susceptibility of the three crystals, showing sharp SC transitions (see Table I). (e) Normalized intensity of the CDW reflections at $\mathbf{Q} = (0,\delta_b,6.5)$ and $(0,2+\delta_b,6.5)$ versus temperature at zero magnetic field ($H = 0$ T) for $y = 6.44$ and 6.512, as well as at $H = 10$ T for $y = 6.44$. (f) δ_b versus temperature for five different dopings. The data sets are limited to temperatures where δ_b could be reliably determined. The inset shows a section of the reciprocal space $(0,k,\ell)$ with the trajectories of typical k scans through the CDW peaks at $\mathbf{Q} = (0,\delta_b,6.5)$ and $(0,2+\delta_b,6.5)$. Data collected at beamline P07: (a) all, (e) all of $H = 10T$ and some of $H = 0T$ for $y = 6.44$, and (f) some for $y = 6.44$. Data collected at beamline 6-ID-D: (b) all, (c) all, (e) some of $H = 0$ T for $y = 6.44$ and all for $y = 6.51$, and (f) some for $y = 6.44$ and all for $y = 6.51$. Data collected at beamline BW5: (f) all for $y = 6.54$, 6.67, and 6.75. Solid lines in (e) and (f) are guides to the eye.

at 6-ID-D with 0.5×0.5 mm^2 beam), and about $1/20$ for the weaker peaks such as for $y = 6.44$ at $T \sim 10$ K. The counting time was adjusted accordingly and varied between 30 and 180 s/point. Compared to LBCO, the background signal of YBCO is larger, while the CDW peaks are broader with similar integrated intensity, resulting in an overall lower signal-to-background ratio for YBCO. Two different sample environments were used: a closed cycle cryostat reaching $T \sim 7$ K, and a magnet cryostat allowing temperatures down to 3 K and magnetic fields up to $H = 10$ T along the c axis of the crystals. Scattering vectors $\mathbf{Q} = (h,k,\ell)$ are specified in units of $(2\pi/a, 2\pi/b, 2\pi/c)$ of the orthorhombic unit cell with space group $Pmmm$. The correlation lengths of the CDW order and the oxygen-chain order in the direction of the b axis are defined by $\xi_b = (\mathrm{HWHM} \times b^*)^{-1}$, where HWHM is the half width at half maximum of the corresponding superstructure reflection.

The results are compared to our previously published work for $y = 6.54$, 6.67, and 6.75, obtained under similar or identical conditions at beamlines BW5 at DORIS III, DESY, and P07.

III. RESULTS

A. Temperature dependence

The CDW order in YBCO leads to weak satellite reflections at wave vectors $\mathbf{Q} = \boldsymbol{\tau} + \mathbf{q}_{\mathrm{CDW}}$ where $\mathbf{q}_{\mathrm{CDW}} = (\delta_a,0,0.5)$ and $(0,\delta_b,0.5)$ are the ordering wave vectors, and $\boldsymbol{\tau}$ a fundamental Bragg reflection [3]. In Figs. 1(a) and 1(b) we show k scans through the position $\mathbf{Q} = (0,\delta_b,6.5)$ for the two ortho-II compositions $y = 6.44$ and 6.512 at different temperatures. Both crystals clearly display a CDW reflection, which makes $y = 6.44$ the composition with the currently lowest reported
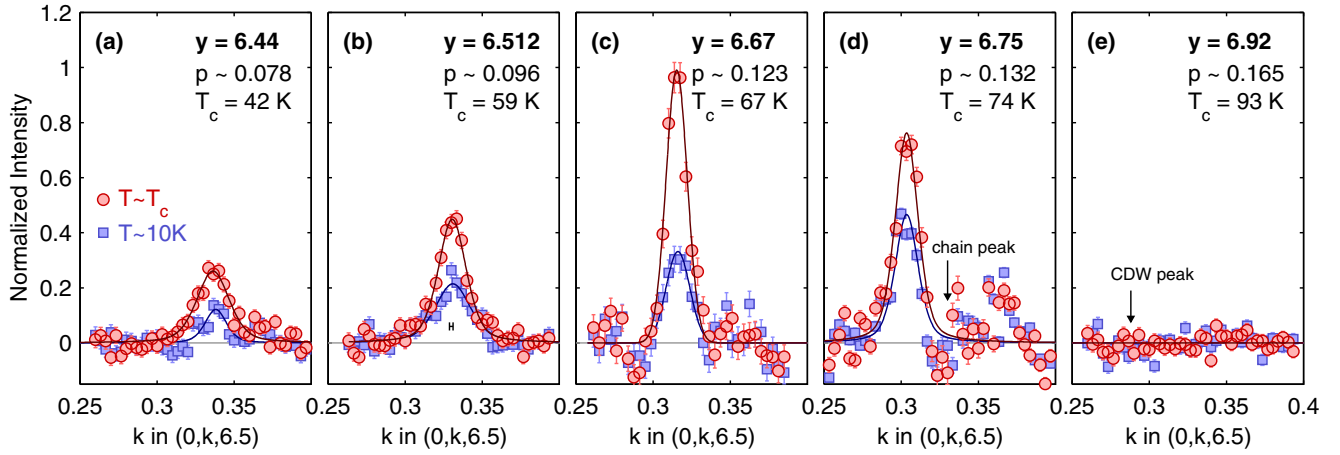
FIG. 2. (Color online) Doping dependence in zero magnetic field of the CDW peak intensity in YBCO. (a)–(e) k scans at $T \sim T_c(y)$ (circles) and $T \sim 10$ K (squares) through the CDW reflection $\mathbf{Q} = (0, \delta_b, 6.5)$ for the oxygen concentrations $y = 6.44$, 6.512, 6.67, 6.75, and 6.92. All intensities are displayed after background subtraction and careful normalization to reflect changes as a function of doping (see text for details). Solid lines through the peaks are least-squares fits using a Gaussian line shape. The horizontal bar in (b) indicates a typical resolution (full width at half maximum). The arrow in (d) marks the position of a subtracted peak from the ortho-III oxygen order in the minority twin domain, which is responsible for the lower statistics in that area. The arrow in (e) shows an estimated CDW peak position as explained in Fig. 1. Examples of data including background counts are given in Refs. [3,46]. All data in this figure were collected at beamline 6-ID-D.

hole concentration with CDW order. In contrast, no evidence of a CDW peak is observed for $y = 6.92$ in Fig. 1(c) in the area of the estimated peak position.

Recent x-ray diffraction studies (resonant [47] and nonresonant [46]) on ortho-II ordered YBCO crystals with $y \sim 6.54$ revealed the existence of CDW reflections along $\mathbf{a}^*$ and $\mathbf{b}^*$. However, in both cases strongly anisotropic structure factors are observed, with CDW satellites along $\mathbf{a}^*$ being generally sparser and weaker than along $\mathbf{b}^*$. In addition the background from the tails of oxygen ordering peaks is larger along $\mathbf{a}^*$. A similar situation is found for the ortho-II crystal with $y = 6.44$. For the ortho-II crystal with $y = 6.512$ no measurements of equivalent CDW peaks in the $(h, 0, \ell)$ zone have been conducted yet. In this paper, we therefore focus on CDW reflections found along $\mathbf{b}^*$.

As can be seen in Fig. 1(e) the temperature dependence for zero magnetic field of the CDW peak intensity for $y = 6.44$ and 6.512 is similar to that previously reported for higher dopings [2,3,46,47]. In the normal state the intensity grows smoothly upon cooling, reaches a maximum at T_c, and then is substantially suppressed in the SC state. For $y = 6.44$, this dependence was consistently measured at $\mathbf{Q} = (0, \delta_b, 6.5)$ and $(0, 2 + \delta_b, 6.5)$. A major difference concerns the onset temperature $T_{\mathrm{CDW}} \sim 90$ K of the CDW order for $y = 6.44$, which is about 50 K lower than for $y \geqslant 6.512$ [46]. Finally, in Fig. 1(f) we show that the incommensurability δ_b for $y = 6.44$ and 6.512 fits well into the existing doping dependence and is approximately independent of temperature for all y.

B. Doping dependence

Next we turn to the doping dependence of the CDW order for zero magnetic field in Fig. 2. For all samples, scans were performed on the CDW reflection $\mathbf{Q} = (0, \delta_b, 6.5)$. Because $6.5c^* \gg \delta_b b^*$, scans along k benefit from the excellent transverse resolution indicated in Fig. 2(b). After lining up on

the nearest Bragg reflection $(0,0,6)$, it is thus straightforward to measure the incommensurability δ_b and the correlation lengths ξ_b of the CDW order with high accuracy [see inset of Fig. 1(f) and Figs. 4(d) and 4(e)]. On the other hand, it is much harder to extract the doping dependence of intensities. For this purpose, we have remeasured five samples—all mounted together on the same sample holder—in a single experiment. The data were normalized in two different ways which led to very similar results: (i) a direct normalization of all intensities by the incident x-ray flux, probed sample volume, and absorption effects, and (ii) a normalization by the integrated intensity of the $(0,0,2)$ Bragg reflection [71], which accounts for the same factors as (i) and is shown in Fig. 2.

For conventional CDW systems, the resulting integrated intensities, I, are proportional to the square of the CDW order parameter Δ, i.e., $\sqrt{I} \propto \Delta(\mathrm{CDW})$ [72]. We would like to normalize $\Delta(\mathrm{CDW})$ so that its maximum value in the YBCO system is 1. Due to the competition with superconductivity, the zero-field, zero temperature value of $\Delta(\mathrm{CDW})$ is less than 1 for all y. However, in the limit $T \to 0$ and in a magnetic field H approaching the upper critical field H_{c2}, it is conceivable to assume $\Delta(\mathrm{CDW}) \sim 1$. For ortho-VIII YBCO with $p = 0.123$, CDW intensities have been measured up to 17 T [3]. This field scale is comparable to $H_{c2} \sim 25$ T reported for this doping [73–77]. The quantity $\sqrt{I(p, T, H)}/\sqrt{I(p = 0.123, 2 \text{ K}, 17 \text{ T})}$ is therefore a good approximation of the doping, temperature, and magnetic field dependence of $\Delta(\mathrm{CDW})$.

The extracted $\Delta(\mathrm{CDW})$ values at zero magnetic field and $T \sim T_c(p)$ as well as $T \sim 10$ K are plotted in Fig. 4(c) versus hole content p. One can see that $\Delta(\mathrm{CDW})$ exhibits a broad maximum at 1/8 doping, and at T_c reaches about 75% of its high-field value at 2 K [3]. As a function of underdoping $\Delta(\mathrm{CDW})$ drops further to about 50% at T_c and 28% at 10 K at the critical point $p_c \sim 0.08$.

Although this clear weakening of the CDW order, as the SDW phase is approached, suggests a competition between the

two phases, the data do not support a complete disappearance of CDW order at p_c. Instead, it suggests a region below p_c where CDW and SDW orders may overlap. To demonstrate this, Fig. 4(c) also shows the volume fraction of the SDW order measured by μSR [78]. At the hole content of our YBa$_2$Cu$_3$O$_{6.44}$ crystal the μSR data suggest a magnetically ordered volume fraction of 25%. The true extent of the overlap depends of course sensitively on the accuracy to which the doping concentration p is determined for the μSR and x-ray experiments. Furthermore, it is well known that the lack of perfect oxygen order at such low oxygen concentrations results in weak sample inhomogeneity [50,51].

A question is therefore whether the weak CDW order in YBa$_2$Cu$_3$O$_{6.44}$ originates from regions with $p > 0.078$ due to inhomogeneity of the hole concentration. There are several facts that speak against this scenario. As can be seen in Fig. 1(e) the CDW intensity peaks right at $T_c = 42$ K. This implies that CDW and SC compete in those parts of the sample where $T_c = 42$ K and, therefore, $p \sim 0.078$. We arrive at the same conclusion based on the doping dependence of the incommensurability δ_b in Figs. 1(f) and 4(d). The fact that δ_b in YBa$_2$Cu$_3$O$_{6.44}$ continues the approximately linear doping trend already reported in Ref. [46] proves that, in those regions with CDW order, p must be close to the estimated value. Finally, Fig. 4(e) shows the correlation length ξ_b measured at $T \sim T_c$. Obviously, ξ_b varies only weakly with doping. Although ξ_b for $y = 0.44$ is slightly lower than for dopings closer to $p = 1/8$, we would expect it to be significantly shorter, if the CDW order were a minority phase. All factors taken together, we conclude that CDW order in YBa$_2$Cu$_3$O$_{6.44}$ is not a result of sample inhomogeneity. Thus, we have demonstrated that intrinsic CDW order exists all the way down to the lower quantum critical point at p_c, where it touches and potentially overlaps with the competing SDW phase [55].

C. Magnetic field dependence

When suppressing SC with a magnetic field of $H = 10$ T applied along the c axis, a significant enhancement of the CDW peak is achieved, as is shown in Fig. 1(e) for $y = 6.44$. The slight drop in intensity below 25 K reflects the fact that 10 T is below the critical field H_{c2} for $y = 6.44$ and thus insufficient to fully suppress SC [77]. This high-field T dependence is very similar to previous observations near 1/8 doping [3,46,47]. To compare the doping dependence of the field effect, we show in Fig. 3 data for the oxygen concentrations $y = 6.44$, 6.512, and 6.67 at $T = 3$ K and $H = 0$ and 10 T. All scans were performed at $\mathbf{Q} = (0, \delta_b, 6.5)$, and have been normalized by the peak intensities in zero field. Independent of the hole content, the application of 10 T along the c axis enhances the CDW peak by a factor of 2.5 to 3. On an absolute scale as in Fig. 2 this means that gains are most significant for $p \sim 1/8$. This seems to correlate with the fact that H_{c2} is minimum at $p = 1/8$ [77].

IV. DISCUSSION

A. Competing CDW and SDW orders near p_c

The underdoped part of the YBCO phase diagram is complex and interesting because several electronic phases
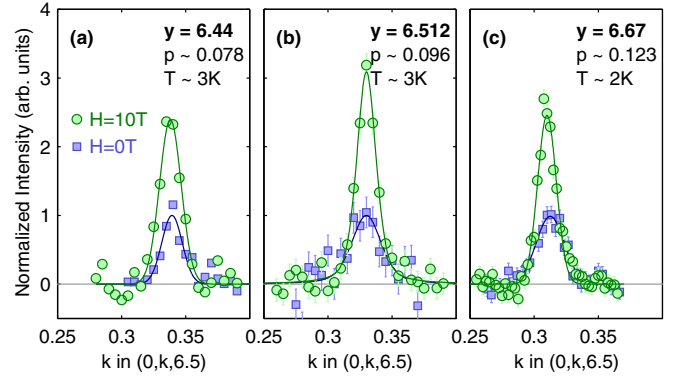

FIG. 3. (Color online) Magnetic field effect on the CDW peak intensity in YBCO at base temperature for concentrations $y = 6.44$, 6.512, and 6.67. (a)–(c) k scans at $H = 0$ and 10 T through $\mathbf{Q} = (0, \delta_b, 6.5)$. For each doping scans have been normalized by the maximum peak intensity in zero magnetic field. Solid lines are least-squares fits using a Gaussian line shape. Sloping backgrounds have been subtracted from all scans. In (a) error bars are within symbol size. All data in this figure were collected at beamline P07.

coexist with superconductivity (see Fig. 5). The SDW order identified by neutron scattering for dopings just above the critical concentration $p \sim 0.05$ of the antiferromagnetic phase, vanishes again in the vicinity of the quantum critical point $p_c \sim 0.08$ [55]. We note that p_c is well inside the SC dome as well as the ortho-II phase, which both set in at $p \sim 0.05$ ($y \sim 6.3$) [14,51,82]. For $p > p_c$ superconductivity was shown to compete with CDW order [1–4,45,48]. In approximately the same doping region centered at $p \sim 1/8$, quantum oscillation experiments [11,14,15] in concert with high-field Hall and thermopower measurements [23,24] were interpreted in terms of an electron pocket. So far, CDW order is the most natural explanation for a Fermi surface reconstruction that produces these pockets [1,18,83].

To make further progress it is obviously critical to understand the region around p_c where CDW crosses over to SDW. If CDW order is connected to the presence of electron pockets, one would naively expect it to weaken significantly across p_c. Our results would support such a scenario. First, the data for $y = 6.44$ and 6.512 confirm that CDW order evolves systematically with underdoping, and persists all the way to $p_c \sim 0.08$. Second, the CDW order for $y = 6.44$ is weakened, although not as drastically as we had expected, and the onset temperature T_{CDW} is substantially reduced. Derived phase diagrams of both the order parameters in Fig. 4(c), and the onset temperatures in Fig. 5 strongly indicate a competition between SDW and CDW phases, which may include a not insignificant region of coexistence. This suggests that the proposed Lifshitz transition at p_c may occur when the CDW order weakens through phase competition.

B. CDW onset temperature

The decrease of T_{CDW} with underdoping is an important observation, because other characteristic temperatures in the underdoped regime, especially the pseudogap temperature T^*, appear to continue to increase with underdoping [10,22,84–88]. To identify properties potentially connected
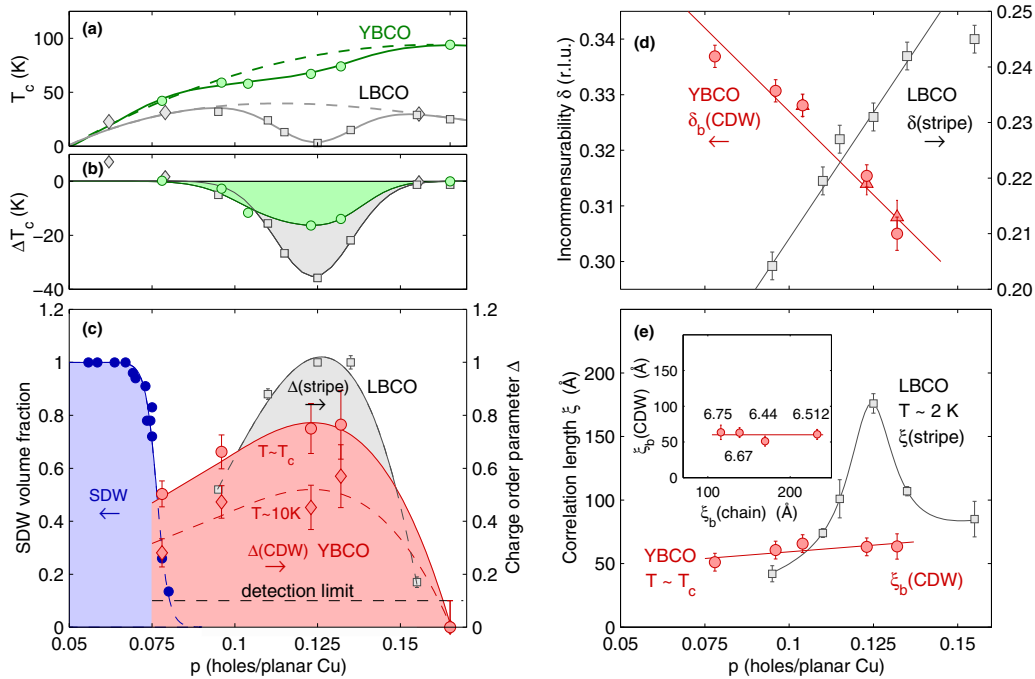
FIG. 4. (Color online) Comparison of CDW order in YBCO with charge stripe order in LBCO as a function of planar hole concentration p for zero magnetic field. (a) Superconducting transition temperature T_c and (b) suppression of T_c through 1/8 effect for YBCO from this work (circles) and Ref. [52] (green lines), and for LBCO from Ref. [79] (diamonds) and Ref. [39] (squares). The dashed gray line in (a) for LBCO is a cubic fit [80] of $T_c(p)$ outside the 1/8 region to describe the envelope of the SC dome, while the solid line includes a Gaussian term to account for the 1/8 anomaly. (c) The right ordinate shows the CDW order parameter Δ(CDW) in YBCO measured at $\mathbf{Q} = (0, \delta_b, 6.5)$ in zero magnetic field, and normalized to the high-field low-temperature value of the ortho-VIII crystal with $y = 6.67$ (see text for details). Red circles were measured at $T \sim T_c(p)$, and red diamonds at $T \sim 10$ K. The solid and dashed red lines are guides to the eye. The left ordinate represents the SDW volume fraction measured by μSR (closed blue circles) [78]. Gray squares indicate the charge stripe order parameter Δ(stripe) in LBCO measured with x rays in zero magnetic field at $T \sim 3$ K [81]. The horizonal dashed line indicates an approximate detection limit for the high-energy x-ray diffraction experiment. We note that panel (c) does not compare the absolute strength of the charge orders in YBCO and LBCO. It compares the order parameters of each of the two systems relative to their individual maximum possible order at 1/8 doping. (d) CDW incommensurability δ_b(CDW) in YBCO measured at $T \sim T_c(p)$ and $\mathbf{Q} = (0, \delta_b, 6.5)$ (red circles) as well as data from Ref. [46] (red triangles). Gray squares indicate the charge stripe incommensurability δ(stripe) in LBCO [39,81]. (e) CDW correlation length ξ_b(CDW) in YBCO measured at $T \sim T_c(p)$ and $\mathbf{Q} = (0, \delta_b, 6.5)$ (red circles), and stripe correlation length ξ(stripe) in LBCO [39,81] at $T \sim 3$ K (gray squares). The resolution has been deconvolved, although it is basically negligible [see Fig. 2(b) and Table I]. The inset shows ξ_b(CDW) of the CDW order versus ξ_b(chain) of the oxygen order, both measured in the direction of the b axis. (d), (e) The data for δ_b(CDW) and ξ_b(CDW) are average values obtained from measurements of the same peak $\mathbf{Q} = (0, \delta_b, 6.5)$ in several beam times (see Table I).

to the CDW order, Fig. 5 shows a critical temperature $T^\dagger$ that marks a broad maximum in the $1/(T_1 T)$ signal of planar ^{63}Cu NQR/NMR experiments [56,65–70]. The agreement between T_{CDW} and $T^\dagger$ is very suggestive. This NQR/NMR feature at $T^\dagger$ is characteristic for samples in the pseudogap phase where $T_c < T^\dagger < T^*$. It is apparent that $T^\dagger$ decreases with underdoping, too. The origin of $T^\dagger$ is a matter of debate, but common interpretations involve the onset of spin freezing, and a gapping of the low-energy spin fluctuations by the pseudogap or by incoherent pairing in the normal state [56,63,68,89,90]. With respect to the incoherent pairing scenario, it is worth noticing yet another property that shares a similar doping dependence as T_{CDW} and $T^\dagger$, and that is the onset temperature reported in Ref. [91] of so-called precursor diamagnetism [92] in the static magnetic susceptibility $\chi(T)$ of YBCO for $H \parallel c$. The discovery of CDW order surrounding the 1/8 anomaly introduces important aspects to this debate. In particular, the peak in the relaxation of the NMR may indicate a response of the spin dynamics to the formation of

the CDW. Associated effects on static magnetic susceptibility and electronic transport coefficients are likely. More work is certainly needed to elucidate such connections. It should be noted that various comparisons of T_{CDW} to other critical temperatures have been reported [3,10,22,88,93].

C. CDW order in YBCO vs stripe order in LBCO

1. Order parameter and incommensurability

The striking similarity of the thermopower response found in YBCO and stripe ordered La-based cuprates suggests that a reconstruction of the Fermi surface into one with small electron pockets may be a universal feature of charge ordered cuprates [23,29,31]. It is therefore interesting to compare the doping evolution of the charge orders in YBCO and the prototypical stripe compound LBCO [39,81,94]. To this end, Fig. 4(a) displays $T_c(p)$ of both systems, clearly showing the well-known suppression of T_c near 1/8 doping [39,52,79]. To quantify the 1/8 anomaly in YBCO, the authors of Ref. [52]
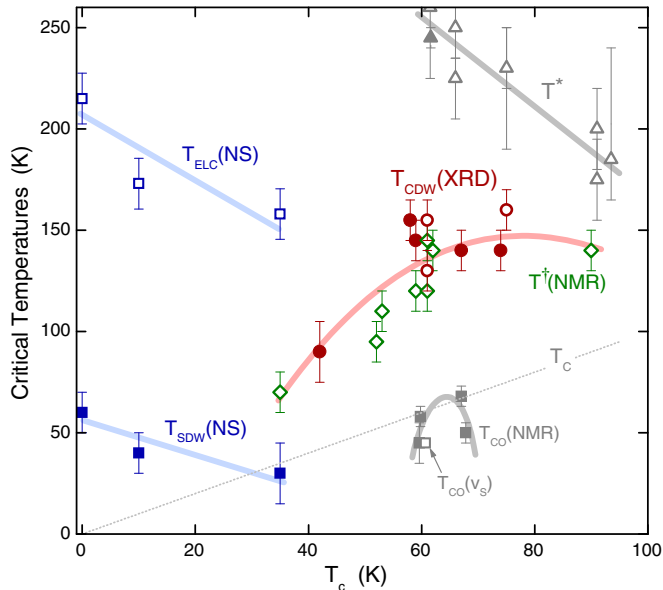
FIG. 5. (Color online) Critical temperatures of competing spin and charge orders in YBCO as a function of T_c. By plotting all data versus T_c, ambiguities of plots versus the planar hole content p, due to different ways and difficulties of determining p, can be reduced [52]. We show the transition temperatures T_{CDW} of CDW order measured by high-energy x rays [3,46] (closed circles) and soft x-ray scattering [2,47,93] (open circles), T_{CO} of charge order detected by high-field NMR [1,68] and high-field sound velocity (v_S) measurements [48], $T^\dagger$ determined from the maximum in $1/(T_1T)$ of planar ^{63}Cu NQR/NMR as explained in the text [56,65–68] (open diamond), the pseudogap temperature T^* as detected by means of Nernst effect (open triangle) and resonant ultrasound measurements [87,88] (closed triangle), T_{SDW} of SDW order (closed blue square), and T_{ELC} of a so-called electronic liquid crystal state as determined by neutron scattering [55,63] (open blue square). T_c is indicated by a dashed line. All solid lines are guides to the eye.

have subtracted $T_c(p)$ from a fit of the envelope of the superconducting dome. Here we do the same for LBCO and plot the difference $\Delta T_c(p)$ for both systems in Fig. 4(b) [80]. Besides the remarkable fact that in both systems the width of the 1/8 anomaly is the same, one can see that LBCO compared to YBCO shows a stronger suppression of T_c. This agrees well with the fact that LBCO also shows the larger charge order parameter [see Fig. 4(c)]. At 1/8 doping charge stripe order in LBCO is already fully developed in zero magnetic field [39,81], while in YBCO the zero-field CDW order is incomplete and thus SC not fully suppressed [22,52].

The different doping dependence in YBCO and LBCO of the charge order incommensurability has already been pointed out [46] but is repeated in Fig. 4(d) to put the new values for $y = 6.44$ and 6.512 into perspective. One can see that $\delta_b(CDW)$ continues the approximately linear doping trend around 1/8 doping all the way down to $p = 0.078$. In the stripe phase the incommensurabilities of the charge and spin orders are coupled, whereas those of the CDW and SDW orders in YBCO seem to be unrelated [39,46,47]. If one considers the doping dependence of $\delta_b(SDW)$ of the SDW order in YBCO, it appears that this order might actually be a relative of the stripe order in La-based cuprates [55,62]. In

this respect it is interesting that Zn doping in YBCO causes a weakening of the CDW state (and as a matter of fact a suppression of the broad maximum of $1/(T_1T)$ in the planar ^{63}Cu NQR/NMR [95,96]) as well as the reappearance of a SDW state at dopings $p \sim 1/8$ [47,97]. This shows that the CDW and SDW orders not only compete with SC, but also with each other. The results for the hole doping dependence of the SDW and CDW phases near p_c in Fig. 4(c) and Fig. 5 support the same idea.

2. Correlation length

Another interesting difference between YBCO and LBCO concerns the doping dependence of the in-plane charge order correlation length ξ. As can be seen in Fig. 4(e) the correlation length of the charge stripe order in $La_{2-x}Ba_xCuO_4$ exhibits a pronounced maximum at $p = 1/8$ of $\xi(stripe) \sim 180$ Å, but drops rapidly by a factor of 3 within a 3% variation of p. In contrast, in YBCO the correlation length $\xi_b(CDW)$ at $T \sim T_c(p)$ is always quite short and varies only weakly for $0.078 \leqslant p \leqslant 0.132$. Moreover, $\xi_b(CDW)$ appears to be independent of the type of oxygen order (ortho-II, VIII, or III), and also independent of the correlation length $\xi_b(chain)$ of the oxygen chain order measured in the same direction $\mathbf{b}^*$ [see inset in Fig. 4(e)]. One could argue that the type of oxygen order should have little effect on $\xi_b(CDW)$, because it only affects the way the chains are arranged along $\mathbf{a}^*$. However, a recent study also finds no effect of the oxygen order on the CDW correlation length along $\mathbf{a}^*$ [98]. A weak maximum of $\xi(CDW)$ at $p \sim 0.12$ has been indicated in Ref. [10], which is less apparent from our data set where each point was obtained in an identical way. At an average we find $\xi_b(CDW) \sim 60$ Å at T_c, which is comparable to $\xi(stripe)$ in LBCO far away from 1/8 doping. Similar correlation lengths have been found in several soft x-ray studies on YBCO, with a weak tendency toward slightly larger values, which may be due to the smaller probed sample volume [2,47,94,99].

The situation is comparable at base temperature in the SC state and zero magnetic field, because $\xi_b(CDW)$ does not change significantly below T_c, as can be seen in Figs. 1(a) and 1(b) and several other studies [2,3,47]. Only when suppressing superconductivity with a magnetic field, can $\xi_b(CDW)$ be increased below T_c. Nevertheless, even for $p \sim 1/8$ and almost complete suppression of superconductivity, $\xi_b(CDW)$ does not exceed ~ 100 Å [3]. On the one hand this shows that the coexistence with superconductivity is one of the factors that limit $\xi_b(CDW)$ in YBCO. On the other hand, the independence of $\xi_b(CDW)$ from the chain superstructures may indicate that local physics plays an important role as well, as will be discussed below.

D. CDW order and oxygen-chain order

The above differences between the charge order superstructures in LBCO and YBCO are not unexpected because of the materials' distinct crystal structures. The absence of chain layers in La-214 materials is certainly the most important difference. In YBCO these chains introduce an orthorhombic distortion that breaks the fourfold rotational symmetry of the CuO_2 planes, which in itself could stabilize a charge order [18,33,45,61,100]. This is quite similar to LBCO where

charge stripe order is most stable in the low-temperature tetragonal (LTT) phase which breaks the rotational symmetry of the individual planes as well [35,39,101]. Interestingly, the correlation length ξ(stripe) of the charge stripe order in LBCO appears unrelated to ξ(LTT) of the LTT phase [100]. Here we have shown that the same is true for ξ_b(CDW) and ξ_b(chain) in YBCO [cf. Fig. 4(e)]. In both systems charge order does not seem to couple in a simple way to the long range structure that breaks the rotational symmetry. In fact, in LBCO with $p = 0.125$ charge stripes even form when the long range ordered LTT phase is absent, i.e., by restoring a fourfold rotational symmetry of the planes at high pressures [100]. In this high-symmetry phase it was found that ξ(stripe) actually matches ξ(LTT) of persisting diffuse peaks from a quenched disorder of local LTT-type distortions [100,102].

Therefore, one might speculate whether in YBCO the CDW order in the planes couples to local rather than long range properties of the chains. In general a coupling of the electronic correlations in the planes and the chains has been a matter of intense debate [56,98,99,103–107]. One of the reasons is that the chains are prone to one-dimensional (1D) -like Peierls instabilities [108]. In fact several scanning tunneling microscopy (STM) studies have identified a modulation of the local density of states along the chains, i.e., along the b axis [103,109]. In agreement with that, a recent soft x-ray angle-resolved photoemission spectroscopy (SX-ARPES) experiment detected a gapped surface chain band whose nesting vector matches the modulation wave vector found by STM [110]. Comparing our bulk sensitive x-ray data results to these surface related observations is not straightforward, since the chain layer at the surface is known to be heavily overdoped [111]. However, both the modulation period ($\sim$9–14 Å) and the correlation length ($\sim$40 Å) reported by STM and SX-ARPES studies [103,109,110] are intriguingly close to our values for δ_b(CDW) and ξ_b(CDW) in Fig. 4. Common interpretations of the charge modulations on the chains are Friedel oscillations [103,109] caused by chain defects, and a Peierls-like CDW instability [110]. The correlation length of the Friedel oscillations, being a local perturbation, may not depend strongly on hole doping or ξ_b(chain). Thus, the almost independence of ξ_b(CDW) observed in our x-ray study is at least not inconsistent with a pinning of the planar CDW order by quenched disorder states on the chains [107]. A recent NMR study arrives at similar conclusions [105]. This discussion shows that both scenarios, a coupling of the planar CDW order to the symmetry breaking potential of well ordered chains, as well as to local chain properties deserve further consideration.

V. CONCLUSIONS

In summary, we have identified CDW order in underdoped YBCO with $y = 6.44$ and 6.512 using high-energy x-ray diffraction. Strong emphasis was placed on the first sample with a hole content $p = 0.078$ that is very close to the critical point p_c. The CDW of this crystal shows the same competition with superconductivity as a function of temperature and magnetic field as previously reported around $p = 1/8$ doping [2,3,45–47]. However, onset temperature and order parameter of the CDW order are significantly reduced. This

implies that CDW also competes with the SDW phase, which becomes the dominant state competing with superconductivity below $p_c \sim 0.08$ [55]. A detailed comparison of the doping dependence of the CDW order in YBCO and the charge stripe order in LBCO is presented. One striking difference is that the correlation length of the CDW order is relatively short ($\sim$60 Å) and almost independent of p, whereas in the case of charge stripe order it shows a pronounced maximum reaching $\sim$180 Å at $p = 1/8$ [39]. Among potential scenarios we consider a coupling between the CDW order in the planes and local states in the chains [103,110]. Furthermore, we find an interesting agreement between the CDW onset temperature and a temperature in nuclear resonance experiments that marks a maximum in the planar relaxation rate [56,65–68]. We argue that the maximum may indicate a response of the low-energy spin fluctuations to the formation of the CDW. When plotted versus a common T_c scale, our results for YBa$_2$Cu$_3$O$_{6.44}$ with $T_c = 42$ K are still slightly above the highest-T_c sample (35 K) with confirmed SDW order [55], and slightly below the lowest-T_c samples with gapped magnetic excitations (48 K) [64] and quantum oscillations (54 K) [112]. This clearly emphasizes that additional doping experiments around p_c are needed to unambiguously determine the relationship between the various competing or coexisting states. Based on our current data, the CDW phase in YBCO exists in a broad doping region which largely overlaps with that characterized by negative transport coefficients and quantum oscillations, thus providing additional support for a potential connection between CDW order and electronlike Fermi pockets [22,23,112]. The only discrepancy is found near p_c, where our data are not inconsistent with a region in which CDW and SDW may coexist, while the negative transport coefficients and quantum oscillations have been reported to disappear [22,23,112]. Although this needs further clarification, the latter properties could be suppressed more strongly by the SDW phase, in particular since they are measured in very high magnetic fields that enhance the SDW order, and may shift p_c to a slightly higher value [54].

Note added in proof. Recently, we became aware of a similar study of the CDW order in YBCO with soft x-ray scattering by Blanco-Canosa *et al.* [113]. The results of the two studies are broadly in agreement.

[1] T. Wu, H. Mayaffre, S. Krämer, M. Horvatić, C. Berthier, W. N. Hardy, R. Liang, D. A. Bonn, and M.-H. Julien, Nature (London) **477**, 191 (2011).

[2] G. Ghiringhelli, M. Le Tacon, M. Minola, S. Blanco-Canosa, C. Mazzoli, N. B. Brookes, G. M. De Luca, A. Frano, D. G. Hawthorn, F. He, T. Loew, M. M. Sala, D. C. Peets, M. Salluzzo, E. Schierle, R. Sutarto, G. A. Sawatzky, E. Weschke, B. Keimer, and L. Braicovich, Science **337**, 821 (2012).

[3] J. Chang, E. Blackburn, A. T. Holmes, N. B. Christensen, J. Larsen, J. Mesot, R. Liang, D. A. Bonn, W. N. Hardy, A. Watenphul, M. v. Zimmermann, E. M. Forgan, and S. M. Hayden, Nat. Phys. **8**, 871 (2012).

[4] T. Wu, H. Mayaffre, S. Krämer, M. Horvatić, C. Berthier, P. L. Kuhns, A. P. Reyes, R. Liang, W. N. Hardy, D. A. Bonn, and M.-H. Julien, Nat. Commun. **4**, 2113 (2013).

[5] E. H. da Silva Neto, P. Aynajian, A. Frano, R. Comin, E. Schierle, E. Weschke, A. Gyenis, J. S. Wen, J. Schneeloch, Z. J. Xu, S. Ono, G. D. Gu, M. Le Tacon, and A. Yazdani, Science **343**, 393 (2014).

[6] R. Comin, A. Frano, M. M. Yee, Y. Yoshida, H. Eisaki, E. Schierle, E. Weschke, R. Sutarto, F. He, A. Soumyanarayanan, Y. He, M. Le Tacon, I. S. Elfimov, J. E. Hoffman, G. A. Sawatzky, B. Keimer, and A. Damascelli, Science **343**, 390 (2014).

[7] N. B. Christensen, J. Chang, J. Larsen, M. Fujita, M. Oda, M. Ido, N. Momono, E. M. Forgan, A. T. Holmes, J. Mesot, M. Hücker, and M. v. Zimmermann, arXiv:1404.3192.

[8] V. Thampy, M. P. M. Dean, N. B. Christensen, Z. Islam, M. Oda, M. Ido, N. Momono, S. B. Wilkins, and J. P. Hill, arXiv:1404.3193.

[9] T. P. Croft, C. Lester, M. S. Senn, A. Bombardi, and S. M. Hayden, Phys. Rev. B **89**, 224513 (2014).

[10] W. Tabis, Y. Li, M. Le Tacon, L. Braicovich, A. Kreyssig, M. Minola, G. Dellea, E. Weschke, M. J. Veit, M. Ramazanoglu, A. I. Goldman, T. Schmitt, G. Ghiringhelli, N. Barišić, M. K. Chan, C. J. Dorow, G. Yu, X. Zhao, B. Keimer, and M. Greven, arXiv:1404.7658.

[11] N. Doiron-Leyraud, C. Proust, D. LeBoeuf, J. Levallois, J.-B. Bonnemaison, R. Liang, D. A. Bonn, W. N. Hardy, and L. Taillefer, Nature (London) **447**, 565 (2007).

[12] A. F. Bangura, J. D. Fletcher, A. Carrington, J. Levallois, M. Nardone, B. Vignolle, P. J. Heard, N. Doiron-Leyraud, D. LeBoeuf, L. Taillefer, S. Adachi, C. Proust, and N. E. Hussey, Phys. Rev. Lett. **100**, 047004 (2008).

[13] J. Singleton, C. de la Cruz, R. D. McDonald, S. Li, M. Altarawneh, P. Goddard, I. Franke, D. Rickel, C. H. Mielke, X. Yao, and P. Dai, Phys. Rev. Lett. **104**, 086403 (2010).

[14] S. E. Sebastian, N. Harrison, and G. G. Lonzarich, Rep. Prog. Phys. **75**, 102501 (2012).

[15] B. Vignolle, D. Vignolles, D. LeBoeuf, S. Lepault, B. Ramshaw, R. Liang, D. A. Bonn, W. N. Hardy, N. Doiron-Leyraud, A. Carrington, N. E. Hussey, L. Taillefer, and C. Proust, C. R. Phys. **12**, 446 (2011).

[16] A. J. Millis and M. R. Norman, Phys. Rev. B **76**, 220503(R) (2007).

[17] N. Harrison and S. E. Sebastian, New J. Phys. **14**, 095023 (2012).

[18] M. Vojta, Physica C **481**, 178 (2012).

[19] Barišić, S. Badoux, M. K. Chan, C. Dorow, W. Tabis, B. Vignolle, G. Yu, J. Béard, X. Zhao, C. Proust, and M. Greven, Nat. Phys. **9**, 761 (2013).

[20] N. Doiron-Leyraud, S. Lepault, O. Cyr-Choinière, B. Vignolle, G. Grissonnanche, F. Laliberté, J. Chang, N. Barišić, M. K. Chan, L. Ji, X. Zhao, Y. Li, M. Greven, C. Proust, and L. Taillefer, Phys. Rev. X **3**, 021019 (2013).

[21] D. LeBoeuf, N. Doiron-Leyraud, J. Levallois, R. Daou, J.-B. Bonnemaison, N. E. Hussey, L. Balicas, B. J. Ramshaw, R. Liang, D. A. Bonn, W. N. Hardy, S. Adachi, C. Proust, and L. Taillefer, Nature (London) **450**, 533 (2007).

[22] D. LeBoeuf, N. Doiron-Leyraud, B. Vignolle, M. Sutherland, B. J. Ramshaw, J. Levallois, R. Daou, F. Laliberté, O. Cyr-Choinière, J. Chang, Y. J. Jo, L. Balicas, R. Liang, D. A. Bonn, W. N. Hardy, C. Proust, and L. Taillefer, Phys. Rev. B **83**, 054506 (2011).

[23] F. Laliberté, J. Chang, N. Doiron-Leyraud, E. Hassinger, R. Daou, M. Rondeau, B. J. Ramshaw, R. Liang, D. A. Bonn, W. N. Hardy, S. Pyon, T. Takayama, H. Takagi, I. Sheikin, L. Malone, C. Proust, K. Behnia, and L. Taillefer, Nat. Commun. **2**, 432 (2011).

[24] J. Chang, R. Daou, C. Proust, D. LeBoeuf, N. Doiron-Leyraud, F. Laliberté, B. Pingault, B. J. Ramshaw, R. Liang, D. A. Bonn, W. N. Hardy, H. Takagi, A. B. Antunes, I. Sheikin, K. Behnia, and L. Taillefer, Phys. Rev. Lett. **104**, 057005 (2010).

[25] A. Hackl, M. Vojta, and S. Sachdev, Phys. Rev. B **81**, 045102 (2010).

[26] M. Sera, Y. Ando, S. Kondoh, K. Fukuda, M. Sato, I. Watanabe, S. Nakashima, and K. Kumagai, Solid State Commun. **69**, 851 (1989).

[27] Y. Nakamura and S. Uchida, Phys. Rev. B **46**, 5841 (1992).

[28] M. Hücker, V. Kataev, J. Pommer, O. Baberski, W. Schlabitz, and B. Büchner, J. Phys. Chem. Solids **59**, 1821 (1998).

[29] T. Noda, H. Eisaki, and S. Uchida, Science **286**, 265 (1999).

[30] T. Suzuki, T. Goto, K. Chiba, M. Minami, Y. Oshima, T. Fukase, M. Fujita, and K. Yamada, Phys. Rev. B **66**, 104528 (2002).

[31] Q. Li, M. Hücker, G. D. Gu, A. M. Tsvelik, and J. M. Tranquada, Phys. Rev. Lett. **99**, 067001 (2007).

[32] J. Zaanen and O. Gunnarsson, Phys. Rev. B **40**, 7391 (1989).

[33] S. A. Kivelson, I. P. Bindloss, E. Fradkin, V. Oganesyan, J. M. Tranquada, A. Kapitulnik, and C. Howald, Rev. Mod. Phys. **75**, 1201 (2003).

[34] J. M. Tranquada, B. J. Sternlieb, J. D. Axe, Y. Nakamura, and S. Uchida, Nature (London) **375**, 561 (1995).

[35] M. Fujita, H. Goka, K. Yamada, J. M. Tranquada, and L. P. Regnault, Phys. Rev. B **70**, 104517 (2004).

[36] M. Hücker, G. D. Gu, J. M. Tranquada, M. v. Zimmermann, H.-H. Klauss, N. J. Curro, M. Braden, and B. Büchner, Physica C **460–462**, 170 (2007).

[37] J. Fink, E. Schierle, E. Weschke, J. Geck, D. Hawthorn, V. Soltwisch, H. Wadati, H.-H. Wu, H. A. Dürr, N. Wizent, B. Büchner, and G. A. Sawatzky, Phys. Rev. B **79**, 100502(R) (2009).

[38] S. B. Wilkins, M. P. M. Dean, J. Fink, M. Hücker, J. Geck, V. Soltwisch, E. Schierle, E. Weschke, G. Gu, S. Uchida, N. Ichikawa, J. M. Tranquada, and J. P. Hill, Phys. Rev. B **84**, 195101 (2011).

[39] M. Hücker, M. v. Zimmermann, G. D. Gu, Z. J. Xu, J. S. Wen, G. Xu, H. J. Kang, A. Zheludev, and J. M. Tranquada, Phys. Rev. B **83**, 104506 (2011).

[40] M. Hücker, Physica C **481**, 3 (2012).

[41] S. Katano, M. Sato, K. Yamada, T. Suzuki, and T. Fukase, Phys. Rev. B **62**, R14677 (2000).

[42] B. Lake, H. M. Rønnow, N. B. Christensen, G. Aeppli, K. Lefmann, D. F. McMorrow, P. Vorderwisch, P. Smeibidl, N. Mangkorntong, T. Sasagawa, M. Nohara, H. Takagi, and T. E. Mason, Nature (London) **415**, 299 (2002).

[43] H.-H. Wu, M. Buchholz, C. Trabant, C. Chang, A. Komarek, F. Heigl, M. v. Zimmermann, M. Cwik, F. Nakamura, M. Braden, and C. Schüßler-Langeheine, Nat. Commun. **3**, 1023 (2012).

[44] L. Taillefer, J. Phys.: Condens. Matter **21**, 164212 (2009).

[45] A. J. Achkar, R. Sutarto, X. Mao, F. He, A. Frano, S. Blanco-Canosa, M. L. Tacon, G. Ghiringhelli, L. Braicovich, M. Minola, M. M. Sala, C. Mazzoli, R. Liang, D. A. Bonn, W. N. Hardy, B. Keimer, G. A. Sawatzky, and D. G. Hawthorn, Phys. Rev. Lett. **109**, 167001 (2012).

[46] E. Blackburn, J. Chang, M. Hücker, A. T. Holmes, N. B. Christensen, R. Liang, D. A. Bonn, W. N. Hardy, M. v. Zimmermann, E. M. Forgan, and S. M. Hayden, Phys. Rev. Lett. **110**, 137004 (2013).

[47] S. Blanco-Canosa, A. Frano, T. Loew, Y. Lu, J. Porras, G. Ghiringhelli, M. Minola, C. Mazzoli, L. Braicovich, E. Schierle, E. Weschke, M. Le Tacon, and B. Keimer, Phys. Rev. Lett. **110**, 187001 (2013).

[48] D. LeBoeuf, S. Krämer, W. N. Hardy, R. Liang, D. A. Bonn, and C. Proust, Nat. Phys. **9**, 79 (2013).

[49] N. Harrison and S. E. Sebastian, New J. Phys. **16**, 063025 (2014).

[50] R. Liang, D. A. Bonn, and W. N. Hardy, Philos. Mag. **92**, 2563 (2012).

[51] M. v. Zimmermann, J. R. Schneider, T. Frello, N. H. Andersen, J. Madsen, M. Käll, H. F. Poulsen, R. Liang, P. Dosanjh, and W. N. Hardy, Phys. Rev. B **68**, 104515 (2003).

[52] R. Liang, D. A. Bonn, and W. N. Hardy, Phys. Rev. B **73**, 180505 (2006).

[53] P. Dai, H. A. Mook, R. D. Hunt, and F. Dogan, Phys. Rev. B **63**, 054525 (2001).

[54] D. Haug, V. Hinkov, A. Suchaneck, D. S. Inosov, N. B. Christensen, C. Niedermayer, P. Bourges, Y. Sidis, J. T. Park, A. Ivanov, C. T. Lin, J. Mesot, and B. Keimer, Phys. Rev. Lett. **103**, 017001 (2009).

[55] D. Haug, V. Hinkov, Y. Sidis, P. Bourges, N. B. Christensen, A. Ivanov, T. Keller, C. T. Lin, and B. Keimer, New J. Phys. **12**, 105006 (2010).

[56] S.-H. Baek, T. Loew, V. Hinkov, C. T. Lin, B. Keimer, B. Büchner, and H.-J. Grafe, Phys. Rev. B **86**, R220504 (2012).

[57] M. R. Norman, Physics **3**, 86 (2010).

[58] M. R. Norman, J. Lin, and A. J. Millis, Phys. Rev. B **81**, 180513 (2010).

[59] V. Hinkov, D. Haug, B. Fauqué, P. Bourges, Y. Sidis, A. Ivanov, C. Bernhard, C. T. Lin, and B. Keimer, Science **319**, 597 (2008).

[60] C. Stock, W. J. L. Buyers, R. A. Cowley, P. S. Clegg, R. Coldea, C. D. Frost, R. Liang, D. Peets, D. Bonn, W. N. Hardy, and R. J. Birgeneau, Phys. Rev. B **71**, 024522 (2005).

[61] S. A. Kivelson, E. Fradkin, and V. J. Emery, Nature (London) **393**, 550 (1998).

[62] M. Fujita, K. Yamada, H. Hiraka, P. M. Gehring, S. H. Lee, S. Wakimoto, and G. Shirane, Phys. Rev. B **65**, 064505 (2002).

[63] V. Hinkov, P. Bourges, S. Phailhès, Y. Sidis, A. Ivanov, C. D. Frost, T. G. Perring, C. T. Lin, D. P. Chen, and B. Keimer, Nat. Phys. **3**, 780 (2007).

[64] S. Li, Z. Yamani, H. J. Kang, K. Segawa, Y. Ando, X. Yao, H. A. Mook, and P. Dai, Phys. Rev. B **77**, 014523 (2008).

[65] M. Takigawa, A. P. Reyes, P. C. Hammel, J. D. Thompson, R. H. Heffner, Z. Fisk, and K. C. Ott, Phys. Rev. B **43**, 247 (1991).

[66] C. Berthier, M.-H. Julien, O. Bakharev, M. Horvatić, and P. Ségransan, Physica C **282–287**, 227 (1997).

[67] T. Auler, M. Horvatić, J. A. Gillet, C. Berthier, Y. Berthier, P. Ségransan, and J. Y. Henry, Phys. Rev. B **56**, 11294 (1997).

[68] T. Wu, H. Mayaffre, S. Krämer, M. Horvatić, C. Berthier, C. T. Lin, D. Haug, T. Loew, V. Hinkov, B. Keimer, and M.-H. Julien, Phys. Rev. B **88**, 014511 (2013).

[69] P. Carretta, Physica C **292**, 286 (1997).

[70] H. Alloul, F. Rullier-Albenque, B. Vignolle, D. Colson, and A. Forget, Europhys. Lett. **91**, 37005 (2010).

[71] To normalize a superstructure reflection it is common to use a nearby fundamental Bragg reflection to maintain a similar scattering geometry. For the CDW peak at $\mathbf{Q} = (0, \delta_b, 6.5)$ that would be $(0,0,6)$. However, if the Bragg reflection is very strong, as is the case for $(0,0,6)$, extinction effects can introduce a significant error to the normalization. Therefore, we have used the much weaker $(0,0,2)$ Bragg reflection. At photon energies on the order of $E_{\mathrm{ph}} = 80$ keV this is possible, because scattering angles are small, and the scattering geometries for $(0,0,2)$ and $(0,0,6)$ not very different.

[72] R. Jaramillo, Y. Feng, J. C. Lang, Z. Islam, G. Srajer, P. B. Littlewood, D. B. McWhan, and T. F. Rosenbaum, Nature (London) **459**, 405 (2009).

[73] Y. Ando and K. Segawa, Phys. Rev. Lett. **88**, 167005 (2002).

[74] J. Chang, N. Doiron-Leyraud, F. Laliberté, R. Daou, D. LeBoeuf, B. J. Ramshaw, R. Liang, D. A. Bonn, W. N. Hardy, C. Proust, I. Sheikin, K. Behnia, and L. Taillefer, Phys. Rev. B **84**, 014507 (2011).

[75] J. Chang, N. Doiron-Leyraud, O. Cyr-Choinière, G. Grissonnanche, F. Laliberté, E. Hassinger, J.-P. Reid, R. Daou, S. Pyon, T. Takayama, H. Takagi, and L. Taillefer, Nat. Phys. **8**, 751 (2012).

[76] B. J. Ramshaw, J. Day, B. Vignolle, D. LeBoeuf, P. Dosanjh, C. Proust, L. Taillefer, R. Liang, W. N. Hardy, and D. A. Bonn, Phys. Rev. B **86**, 174501 (2012).

[77] G. Grissonnanche, O. Cyr-Choinière, F. Laliberté, S. R. de Cotret, A. Juneau-Fecteau, S. Dufour-Beauséjour, M.-E. Delage, D. LeBoeuf, J. Chang, B. J. Ramshaw, D. A. Bonn, W. N. Hardy, R. Liang, S. Adachi, N. E. Hussey, B. Vignolle, C. Proust, M. Sutherland, S. Krämer, J.-H. Park, D. Graf, N. Doiron-Leyraud, and L. Taillefer, Nat. Commun. **5**, 3280 (2014).

[78] S. Sanna, G. Allodi, G. Concas, A. D. Hillier, and R. De Renzi, Phys. Rev. Lett. **93**, 207001 (2004).

[79] N. Yamada and M. Ido, Physica C **203**, 240 (1992).

[80] We note that the envelope of the SC dome of LBCO is asymmetric, and cannot be fit with a quadratic function centered at optimum doping ($p = 0.16$) as is the case in YBCO. Instead we have used a third order polynomial that peaks around $p = 0.12$.

[81] M. Hücker, M. v. Zimmermann, Z. J. Xu, J. S. Wen, G. D. Gu, and J. M. Tranquada, Phys. Rev. B **87**, 014501 (2013).

[82] Y. Ando, S. Komiya, K. Segawa, S. Ono, and Y. Kurita, Phys. Rev. Lett. **93**, 267001 (2004).

[83] H. Yao, D.-H. Lee, and S. A. Kivelson, Phys. Rev. B **84**, 012507 (2011).

[84] B. Fauqué, Y. Sidis, V. Hinkov, S. Pailhès, C. T. Lin, X. Chaud, and P. Bourges, Phys. Rev. Lett. **96**, 197001 (2006).

[85] H. A. Mook, Y. Sidis, B. Fauqué, V. Balédent, and P. Bourges, Phys. Rev. B **78**, 020506 (2008).

[86] J. Xia, E. Schemm, G. Deutscher, S. A. Kivelson, D. A. Bonn, W. N. Hardy, R. Liang, W. Siemons, G. Koster, M. M. Fejer, and A. Kapitulnik, Phys. Rev. Lett. **100**, 127002 (2008).

[87] R. Daou, J. Chang, D. LeBoeuf, O. Cyr-Choinière, F. Laliberté, N. Doiron-Leyraud, B. J. Ramshaw, R. Liang, D. A. Bonn, W. N. Hardy, and L. Taillefer, Nature (London) **463**, 519 (2010).

[88] A. Shekhter, B. J. Ramshaw, R. Liang, W. N. Hardy, D. A. Bonn, F. F. Balakirev, R. D. McDonald, J. B. Betts, S. C. Riggs, and A. Migliori, Nature (London) **498**, 75 (2013).

[89] V. J. Emery, S. A. Kivelson, and O. Zachar, Phys. Rev. B **56**, 6120 (1997).

[90] In general planar ^{63}Cu NQR/NMR experiments are suited to sort out whether the decrease of $1/(T_1 T)$ below $T^\dagger$ is caused by spin freezing or the gapping of low-energy spin fluctuations. Spin freezing becomes dominant at low doping and causes a broadening and weakening of the low-temperature spectra, which is the so-called wipeout effect. This is not the case at higher hole concentrations and temperatures $T_c < T < T^\dagger$ [56]. However, in the intermediate doping range it can be difficult to distinguish these effects. Relaxation rates may drop because of a gap, or because spins, fluctuating at frequencies that cause strong relaxations, freeze-out first. In Fig. 4 we show a significant number of points between $T_c = 52$ and 62 K, which we count among the high-doping regime, and clearly show a decrease of $T^\dagger$ with underdoping. According to Ref. [68], in the sample with $T_c = 35$ K and $T^\dagger = 70$ K, which is most affected by spin freezing, $T^\dagger$ is assumed to still be above the onset temperature of the wipeout effect.

[91] I. Kokanović, J. R. Cooper, and K. Iida, Europhys. Lett. **98**, 57011 (2012).

[92] L. Li, Y. Wang, S. Komiya, S. Ono, Y. Ando, G. D. Gu, and N. P. Ong, Phys. Rev. B **81**, 054510 (2010).

[93] M. Bakr, S. M. Souliou, S. Blanco-Canosa, I. Zegkinoglou, H. Gretarsson, J. Strempfer, T. Loew, C. T. Lin, R. Liang, D. A. Bonn, W. N. Hardy, B. Keimer, and M. Le Tacon, Phys. Rev. B **88**, 214517 (2013).

[94] V. Thampy, S. Blanco-Canosa, M. García-Fernández, M. P. M. Dean, G. D. Gu, M. Först, T. Loew, B. Keimer, M. Le Tacon, S. B. Wilkins, and J. P. Hill, Phys. Rev. B **88**, 024505 (2013).

[95] M.-H. Julien, T. Fehér, M. Horvatić, C. Berthier, O. N. Bakharev, P. Ségransan, G. Collin, and J.-F. Marucco, Phys. Rev. Lett. **84**, 3422 (2000).

[96] T. Timusk and B. Statt, Rep. Prog. Phys. **62**, 61 (1999).

[97] A. Suchaneck, V. Hinkov, D. Haug, L. Schulz, C. Bernhard, A. Ivanov, K. Hradil, C. T. Lin, P. Bourges, B. Keimer, and Y. Sidis, Phys. Rev. Lett. **105**, 037207 (2010).

[98] A. J. Achkar, X. Mao, C. McMahon, R. Sutarto, F. He, R. Liang, D. A. Bonn, W. N. Hardy, and D. G. Hawthorn [Phys. Rev. Lett. (to be published)], arXiv:1312.6630.

[99] A. J. Achkar, F. He, R. Sutarto, J. Geck, H. Zhang, Y.-J. Kim, and D. G. Hawthorn, Phys. Rev. Lett. **110**, 017001 (2013).

[100] M. Hücker, M. v. Zimmermann, M. Debessai, J. S. Schilling, J. M. Tranquada, and G. D. Gu, Phys. Rev. Lett. **104**, 057004 (2010).

[101] Y.-J. Kim, G. D. Gu, T. Gog, and D. Casa, Phys. Rev. B **77**, 064520 (2008).

[102] G. Fabbris, M. Hücker, G. D. Gu, J. M. Tranquada, and D. Haskel, Phys. Rev. B **88**, 060507 (2013).

[103] D. J. Derro, E. W. Hudson, K. M. Lang, S. H. Pan, J. C. Davis, J. T. Markert, and A. L. de Lozanne, Phys. Rev. Lett. **88**, 097002 (2002).

[104] Z. Yamani, B. W. Statt, W. A. MacFarlane, R. Liang, D. A. Bonn, and W. N. Hardy, Phys. Rev. B **73**, 212506 (2006).

[105] T. Wu, H. Mayaffre, S. Krämer, M. Horvatić, C. Berthier, W. N. Hardy, R. Liang, D. A. Bonn, and M.-H. Julien, arXiv:1404.1617 (2014).

[106] E. G. Dalla Torre, Y. He, D. Benjamin, and E. Demler, arXiv:1312.0616.

[107] L. Nie, G. Tarjus, and S. A. Kivelson, Proc. Natl. Acad. Sci. USA **111**, 7980 (2014).

[108] G. Grüner, in *Density Waves in Solids*, edited by D. Pines, Frontiers in Physics Vol. 89 (Addison-Wesley, Reading, MA, 1994).

[109] M. Maki, T. Nishizaki, K. Shibata, and N. Kobayashi, Phys. Rev. B **65**, 140511 (2002).

[110] V. B. Zabolotnyy, A. A. Kordyuk, D. Evtushinsky, V. N. Strocov, L. Patthey, T. Schmitt, D. Haug, C. T. Lin, V. Hinkov, B. Keimer, B. Büchner, and S. V. Borisenko, Phys. Rev. B **85**, 064507 (2012).

[111] M. A. Hossain, J. D. F. Mottershead, D. Fournier, A. Bostwick, J. L. McChesney, E. Rotenberg, R. Liang, W. N. Hardy, G. A. Sawatzky, I. S. Elfimov, D. A. Bonn, and A. Damascelli, Nat. Phys. **4**, 527 (2008).

[112] S. E. Sebastian, N. Harrison, M. M. Altarawneh, C. H. Mielke, R. Liang, D. A. Bonn, W. N. Hardy, and G. G. Lonzarich, Proc. Natl. Acad. Sci. USA **107**, 6175 (2010).

[113] S. Blanco-Canosa, A. Frano, E. Schierle, J. Porras, T. Loew, M. Minola, M. Bluschke, E. Weschke, B. Keimer, and M. Le Tacon, Phys. Rev. B **90**, 054513 (2014).